Milligan 12.3" f/4.1 (Part 1)
Interferometry Comparison

Stephen C. Koehler
steve_koehler@securecomputing.com

June 2005

1   Introduction

This is the first in a series of two articles on tests performed on Scott Milligan's 12.3" f/4.1 mirror. This article compares the results of three independent interferometric analyses. A follow-on article will address the Foucault test results and compare them to interferometry. I chose to treat interferometry separately for two reasons. First, we have a rare opportunity to closely examine the work of two prominent mirror makers (John Hudek of *Galaxy Optics* and James Mulherin of *Optical Mechanics/Torus*). Second, the interferometry on this mirror makes an interesting story in itself, because of the nature of the mirror aberrations and how test stand astigmatism affected the analysis. As you will see, other than a discrepancy in the magnitude of primary astigmatism (probably affected by test stand effects) the end results are strikingly similar.

To keep this article understandable by an audience interested in how interferometry performs, but not well versed in its intricacies, I have written it entirely in non-mathematical terms. Nevertheless, it is helpful to be familiar with basic optical testing concepts, such as, Strehl ratio, spherical aberration, and Foucault test.

This test was by no means just an easy opportunity for Mulherin and Hudek to advertise their expertise in interferometry. A number of characteristics of this mirror presented challenges. First, the mirror is coated, which poses difficulties on an interferometer set up to handle uncoated optics. The reason is that there needs to be a good intensity match between the test and reference beams in the interferometer for measurable fringes to appear. I believe Hudek had never tested a coated optic, and used an ad-hoc technique suggested by someone on the ATM e-mail list to attenuate the test beam by passing it through a piece of lens tissue. Mulherin has a separate interferometer for use with coated optics, but he struggled to get good contrast in the fringes, so his analysis was done on interferograms of very poor image quality.

Second, this mirror was of a smaller size than Hudek's test stands usually hold, so the mirror was held in a temporary stand with less than ideal characteristics. As a result, test stand induced deformation was very large. Mulherin used his normal stand for testing 12.5" optics, but for some reason test stand effects were also large.

Finally, the mirror is relatively fast at f/4.1. This posed difficulties for Eason, who tests without nulling optics. A fast mirror results in highly curved fringes that bunch up at the edge of the interferograms, making them hard to measure accurately. (See the rightmost interferogram in Figure 1.)

As you can see, each optician had some hurdles to cross in testing this optic. Keep this in mind when you see how close the final results were.

Figure 1: Sample Interferograms (Mulherin, Hudek, Eason)
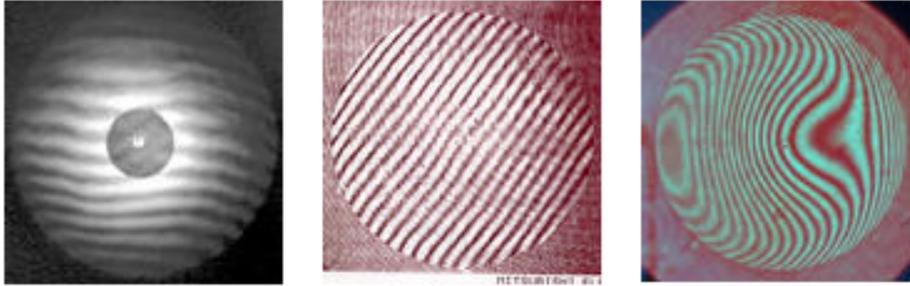
1.1 Background

This article resulted from discussions on the ATM and atm_free e-mail lists regarding apparent differences between interferometry and Foucault tests on some mirrors. As a contribution to the discussion, Scott Milligan offered to make his 12.3" f/4.1 mirror available for independent testing. James Mulherin (Optical Mechanics/Torus) and John Hudek (Galaxy Optics) offered to test the mirror interferometrically with their professional setups. Dale Eason offered to test the mirror with his amateur interferometer and robotic Foucault setups. Besides the original question of why Foucault does not always agree with interferometry, this has resulted in an unusual and exciting opportunity to critically compare the interferometry of two prominent large-mirror makers.

To back up a bit, Scott Milligan offered data on this mirror in support of my contention that the Foucault test seems to report a larger correction error (spherical aberration) on some mirrors compared to interferometry. Scott's original data on this mirror included three sets of interferometry performed with different techniques and equipment and two independent sets of Foucault readings. This mirror follows the pattern I observed, but to a somewhat milder degree than some other examples.

Adding in the new tests, this gives six independent interferometric tests and four independent Foucault tests on this mirror to compare. This report only includes the three new interferometric analyses, because a proper analysis of astigmatism requires interferograms taken in two orientations, which was not done in the earlier interferometry. The follow-on report will include all the interferometric results.

2 Interferometry in General

In general, an interferometer works by causing a "test beam" of light that reflects off the entire surface of the optic under test to interact with a "reference beam" of known quality. When one beam is "tilted" with respect to the other, it results in a visible fringe pattern that can be captured with a camera for analysis. Figure 1 shows some sample interferograms of Scott's mirror.

A typical method of analysis is to use a combination of sofware and manual control to locate many points (hundreds to low thousands) on the centers of the fringes, then use a mathematical technique (least squares fitting) to derive a model of the surface under test. The surface is modeled by way of Zernike polynomials which represent the optical surface by a small number of coefficients (numbers), typically around 36.

Once a Zernike representation is achieved, a wavefront map of the optic can be plotted, and various metrics, such as peak-to-valley (P-V) error, root-mean-square (RMS) error, and Strehl ratio can be derived. The Zernike representation also allows various transformations to be performed on the optical representation, such as rotating or flipping it, and cancelling aberrations inherent in the interferometer setup, such as tilt, defocus, coma, and (sometimes) astigmatism.

If the interferometer setup does not include the use of nulling optics to remove the spherical aberration present in the wavefront from a paraboloidal optic viewed at the center of curvature (COC), then this can also be removed artificially from the Zernike coefficients. Two null setups mentioned in this report are a Ross null lens (which goes between the interferometer and the optic under test), and a large autocollimation flat, which makes it possible to perform the interferometry at focus, instead of the center of curvature. Both these null setups remove the spherical aberration optically, and the resulting interferograms should have relatively straight fringes, as seen in the two leftmost samples in Figure 1. The autocollimation flat doubles the sensitivity of the interferometer, because the test beam bounces off the optic twice.

One test-induced defect that needs to be mentioned is test stand astigmatism[1]. For practical reasons, mirrors are usually tested on edge in some sort of test stand. Mirrors held this way typically sag in a characteristic way, with the top and bottom of the mirror flopping forward and the sides of the mirror flopping back. Interferometry, which measures the entire 2D surface of the mirror, must somehow account for test stand astigmatism, which can easily swamp the small aberrations you are trying to measure. One way to do this is to artificially cancel all primary astigmatism in the analysis. However, if this is not done with care, it can cause you to miss astigmatism present on the optical surface.

A better way to account for test stand astigmatism in the analysis is to take two sets of interferograms, one set with the mirror in one orientation (A), and one set with the mirror rotated 90 degrees (B). In the analysis, if you counter-rotate the B set to match the mirror orientation of the A set and average, you will tend to cancel test induced astigmatism while leaving any astigmatism inherent in the optical figure.[2]. This is an approximate method, because actual test stand astigmatism is more complex than pure primary astigmatism, so the cancellation may not be perfect. Fortunately, all three interferometrists took such double sets of data, so astigmatism could be analyzed.

3   Equipment and Techniques

This section describes the interferometers and associated equipment used to perform the tests in this article. Tables 1, 2, and 3 give the details of both the interferometry and and the analysis. One general comment on the interferometry is that the tests were so completely independent— the only thing in common was the mirror under test. Specifically, they used different test stands, interferometers, nulling optics, test operator, and analysis software. In the case of Hudek and Eason, I started with the Zernike terms. In the case of Mulherin, I decided to retrace the interferogram fringes and derive the Zernike terms myself.

---

[1]By "test stand astigmatism" I mean all test-stand induced aberrations, which often include more than pure primary astigmatism.

[2]This technique will also cancel any astigmatism caused by the interferometer. For example, the Bath interferometer used by Eason introduces a small amount of astigmatism, because the test and reference beams are slightly off-axis.
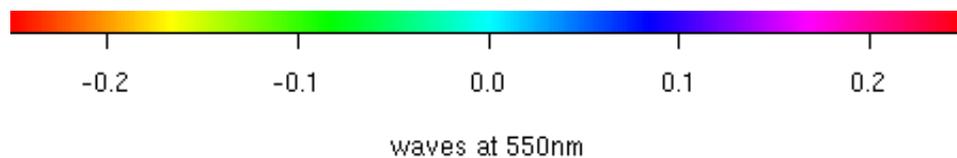
Figure 2: Wavefront Map Scale

waves at 550nm

Table 1: Hudek Equipment/Techniques

| Interferometery	
Operator	John Hudek
Type	Fizeau with lens tissue beam attenuator for coated optic
Source	HeNe laser Stabilized/Polarized @ 632.8nm
Reference Element	Diameter: 32mm f3.5, RC: 81.64mm CV, PVWF: 0.057, RMS: 0.009, Clear aperture test area: 100%, Mounted clear aperture: 30mm, AR coated
Nulling Optics	Ross Null Lens, Diameter: 102mm, Type: Plano/Convex, Material: BK-7, RC: 270.32mm, Usable clear aperture: 85mm (Typical use aperture based on the test optic diameter and focal ratio: 35mm to 85mm or 35% to 85%), Plano: PVWF: 0.044/RMS: 0.006, Radius: PVWF: 0.055/RMS: 0.010, AR coated
Imaging Device	"Watec" Model: WAT-308 B&W CCD Camera with 16mm 1:1.4, Frame Grabber
Interferograms	5 in orientation A, 5 in orientation B, various fringe orientations and tilt
Test Stand	50 degree pegs with mirror vertical
Analysis	
Type	Fringe tracing
Operator	John Hudek
Analysis Program	Phase Shift Technology "Fastvai" Version 3.17, 1999
Zernike Set	36 terms, including an extra symmetric term without the associated asymmetric terms (QuickFringe set), reported as waves at 550nm
Postprocessing	Flip x-axis to account for reflection in interferometer.

Table 2: Mulherin Equipment/Techniques

Interferometery	
Operator	James Mulherin
Type	Fizeau (Shack cube)
Source	Stabilized laser @ 532nm
Reference Element	Certified to about 1/20th wave P-V at F/2 using a Zygo interferometer at Tucson Optical Research Corp. Scott's mirror used only the central f/4 portion, which should be significantly better than 1/20th wave.
Nulling Optics	30" perforated flat, 1/10 wave P-V across the full diameter. This test used only the central 12.3".
Imaging Device	Integral Technologies FlashBus MV
Interferograms	5 in orientation A, 5 in orientation B, similar fringe orientations and tilt
Test Stand	90 degree pegs with mirror vertical against three support points
Analysis	
Type	Fringe tracing
Operator	Steve Koehler
Analysis Program	FringeXP for fringe tracing, my own R tools for the Zernike fit
Zernike Set	49 terms reported in source waves, both light and dark fringes were traced
Postprocessing	Rotate 180 degrees, scale from 532nm to 550nm

Table 3: Eason Equipment/Techniques

Interferometery	
Operator	Dale Eason
Type	Bath
Source	Red laser pointer @ 630nm
Reference Element	none
Nulling Optics	none
Imaging Device	web cam with frame grabber
Interferograms	40 total in orientations A and B with a variety of fringe orientations
Test Stand	90 degree pegs with mirror tilted back slightly
Analysis	
Type	Fringe tracing
Operator	Dale Eason
Analysis Program	OpenFringe
Zernike Set	39 terms, including three extra symmetric terms
Postprocessing	Flip x-axis, scale from 630nm to 550nm, artificially remove spherical aberration for test setup (artificial null)

Figure 3: Individual Mulherin Results
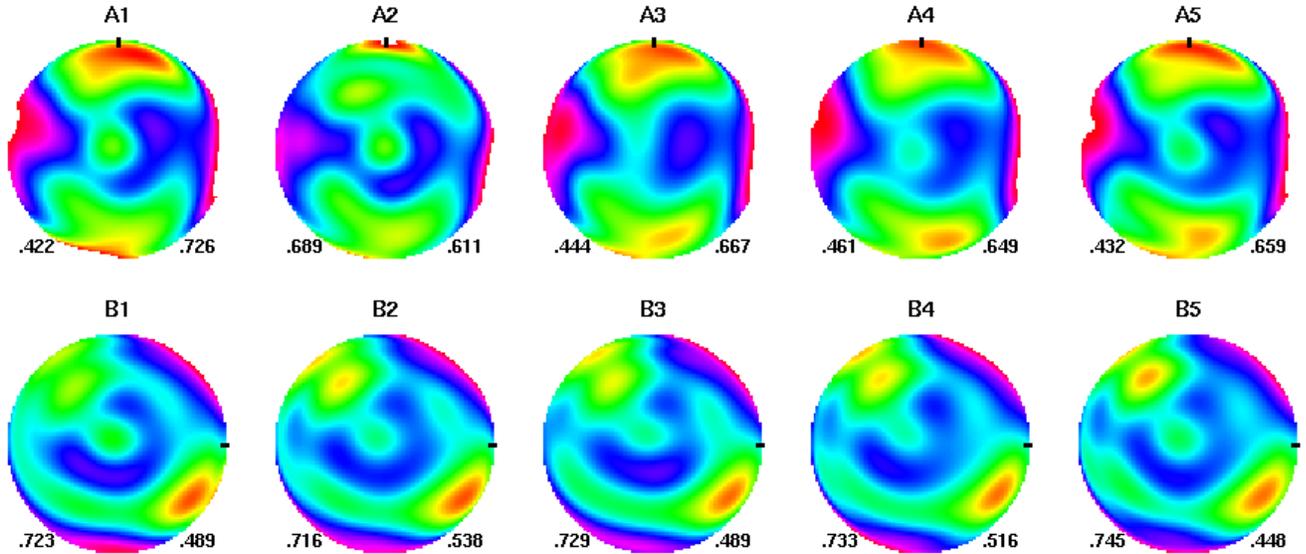

3.1 Notes

- Hudek used a piece of lens tissue stretched across the test beam to equalize the intensity with the reference beam. From the appearance of the interferograms, it seems to have worked very well. The effect on the results is unknown.

- Mulherin performed the interferometry with the optic in auto-collimation using a perforated flat. This results in a 25% "obstruction" in the interferograms, which means that no data could be taken on the middle of the mirror. The other testers were able to measure the middle of the mirror.

- Eason's setup without the use of nulling optics means that the spherical aberration from testing at the center of curvature needed to be removed artificially from the Zernike terms. Doing this requires accurate measurement of the source wavelength, mirror diameter and the radius of curvature, and accurate delimiting of the edge of the mirror in interferogram analysis. Inaccuracy in these can throw off the measurement of spherical aberration in the results. (This is a disadvantage of not using nulling optics.)

4 Results

As a starting point, let's look at the wavefront maps for individual interferograms taken by Mulherin. Figure 2 shows wavefront maps of all ten individual interferograms. The aberrations termed piston, tilt, defocus, and coma have been artificially removed from the data, because they have to do with the interferometer itself, not the test optic.

The wavefront maps in this paper use a uniform color scale, as shown in Figure 2. It spans the range $-1/4\lambda$ to $1/4\lambda$ at 550nm, with light blue at the middle of the scale. Darker blue represents

Figure 4: Averaged Interferogram Sets
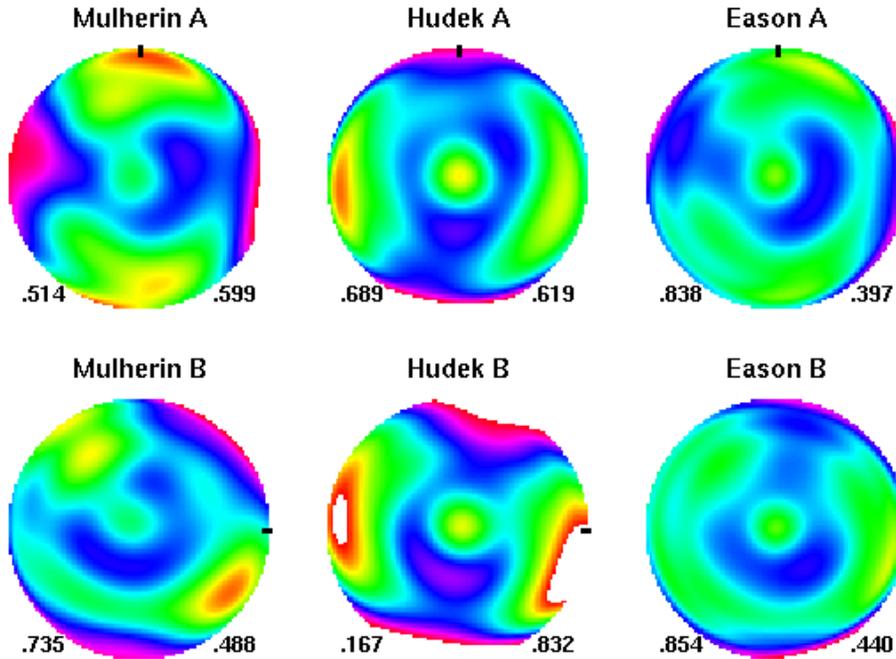
high regions, and green represents low regions. The wavefront maps have been annotated with Strehl ratio on the left and P-V error on the right. When applicable, an index mark indicates the "top" of the mirror, which is at the 12 o'clock position for test orientation A and at the 3 o'clock position for test orientation B.

Note that there is a lot of similarity within set A and within set B, but there are a lot of differences between the sets. Individual frame-to-frame differences are due to vibration and air currents in the test chamber and random fringe measurement error. The big differences between the sets A and B are the mark of test stand astigmatism, which almost completely swamps the results. (As shown below, test stand astigmatism for Mulherin was greater than $1/4\lambda$ P-V error on the wavefront, which is typical for testing mirrors on edge.)[3]

The first step of analysis is to average the results within the data sets to cancel the random effects of vibration, air currents, and fringe measurement errors. Figure 4 shows the results averaging sets A and B from the three interferometrists. From this, it is clear that the test stand had drastically different effects for the three participants. Hudek's results show a typical test stand sag, where the top and bottom of the mirror are deformed upward (blue), and the sides downward (green). For some reason, Mulherin's results show a similar amount of astigmatism, but in a reverse mode. Eason used a test stand that was tilted back somewhat, almost completely eliminating test stand astigmatism. Only in Eason's results do the actual asymmetric shape of this mirror start to

---

[3]Actually, with a diameter to thickness ratio of 6:1, Scott's mirror is classified as a full-thickness mirror. I was a bit surprised at the amount of test stand astigmatism that showed up. However, it must be noted that the goal of these tests were to collect data for comparison with Foucault, not strive for individually perfect interferometric results.
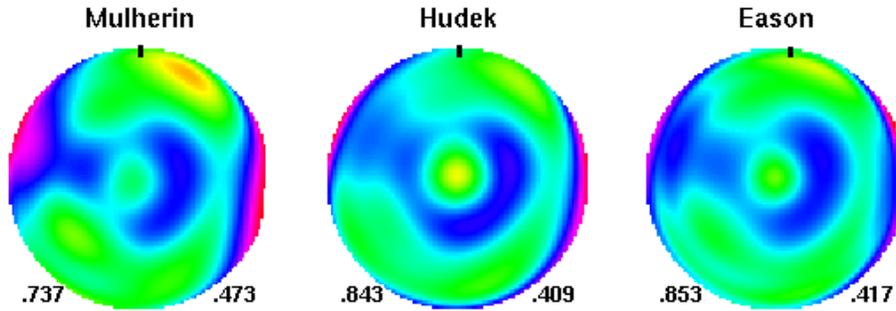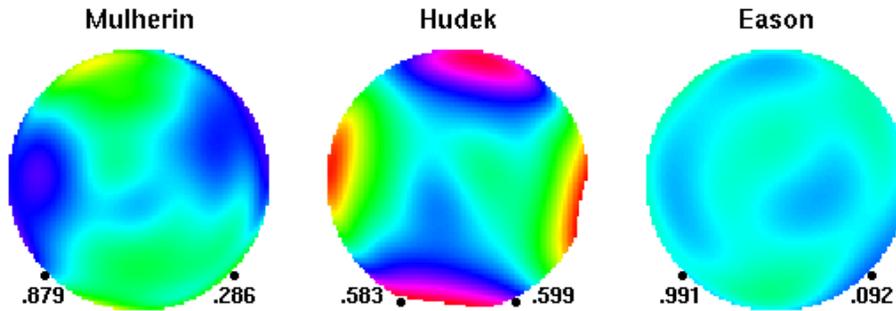
Figure 5: Test Stand Removed


Figure 6: Test Stand Aberrations (Method 1)

emerge—notice how the "ring with ridge to the edge" rotates between set A and B. In Mulherin's and Hudek's results (so far) the shape of the mirror is almost completely obscured by test stand effects.

The next step in analysis is to remove test stand astigmatism, since it otherwise overshadows the mirror aberrations. Often, a shortcut of simply canceling the Zernike term for primary astigmatism is justified, if other tests show little astigmatism on the optic. In this case, however, we have two data sets taken with the optic rotated 90 degrees, which permits us to analyze for test stand astigmatism directly. The result of using a counter-rotate and average to cancel test stand astigmatism is shown in Figure 5.

Finally, the results of the three interferometerists are looking similar, in fact, strikingly similar. It can clearly be seen in Figure 5 that the same pattern (a circular hill with a ridge to the edge) is present in all images. Notice that Hudek's results appear to be rotated a bit clockwise with respect to the others. I will address this, below. The biggest difference between these results is that the Strehl ratio from Mulherin is significantly lower than the other two (.737, versus, .850). This explore this further, below.

Instead of cancelling test stand astigmatism, there are a variety of techniques available to capture what it looks like. This is instructive to do, especially since we have the opportunity to compare three independent tests with different support systems. I used a method which extracts the test

8

Figure 7: Zernike Term Comparison
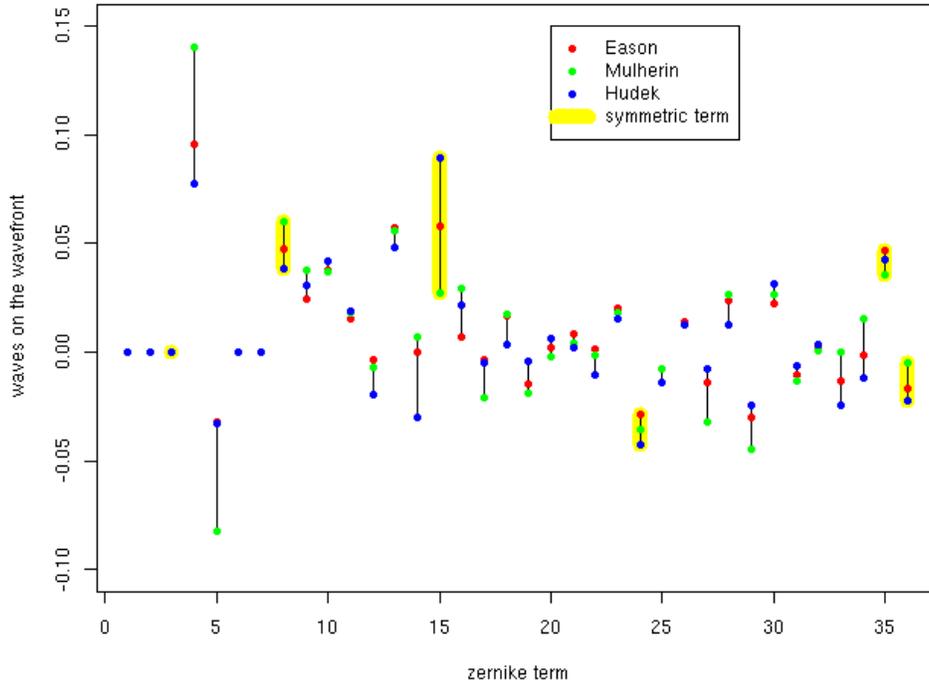
stand deformation from the averages of the Zernike terms for sets A and B. See Figure 6. I have added the location of the test stand pegs to wavefront maps. In general, the test stand deformations are aligned vertically, but as you can see, Mulherin's is the reverse of Hudek's. It is also interesting to see that test stand astigmatism is not pure primary astigmatism (which is saddle-shaped), but has some higher-order terms mixed in (asymmetry in the aberrations). I suspect that this is typical of test stand astigmatism in large, thin mirrors seen today. Note that small clockwise rotation is present in Hudek's test stand astigmatism, which corresponds to the rotation seen in Figure 5.

Next, let's try to explain the lower Strehl ratio for Mulherin's results. For this purpose, it is instructive to compare the Zernike terms directly, to try to understand the exact nature of the differences. Figure 7 does this graphically[4]. For the most part, the Zernike terms track very well among the results from the three interferometrists. Personally, I was surprised to see the results track well out into the higher-order terms. The biggist differences are in the terms for primary astigmatism (terms 4 and 5), and the term for the first higher-order spherical aberration (term 15). In particular, Mulherin's astigmatism terms (green) are larger than the other two (red, blue), which track fairly well.

I have a guess about what caused the discrepancy in the astigmatism term. Because we have independent confirmation of mirror wavefront (Eason and Hudek agree very well), we can use this to derive the test stand astigmatism for orientations A and B, separately. Figure 8 shows the results of subtracting Eason's final wavefront from the original averages of sets A and B. For this figure, I also took the liberty of adjusting the rotation of Hudek's results to make the astigmatism line up

---

[4]In the Zernike comparison, I adjusted Hudek's results by a small rotation, explained below. Not doing this introduces apparent discrepancies in the asymmetric terms that are purely the result of rotation.

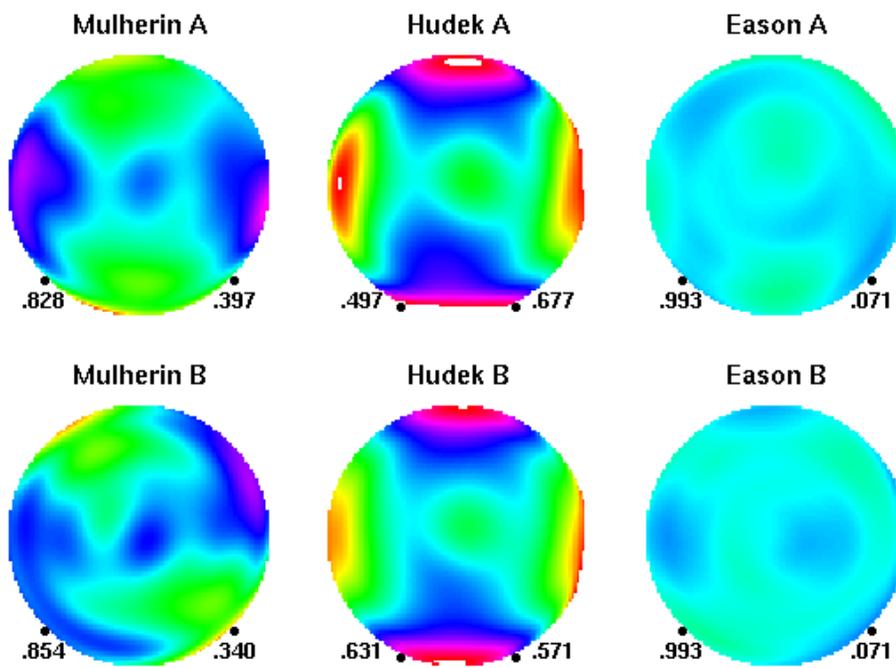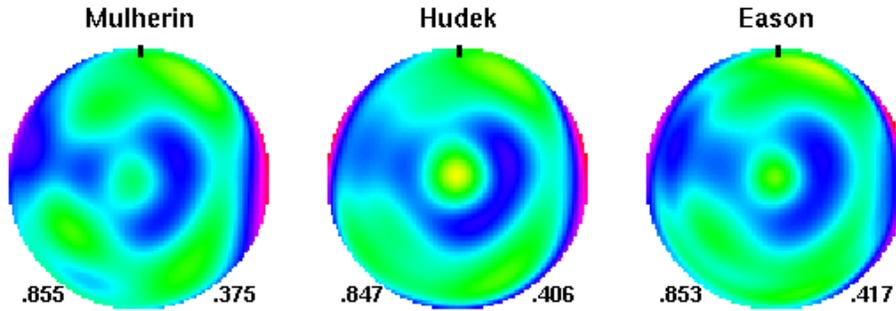Figure 8: Test Stand Aberrations (Method 2)

Figure 9: Final Adjusted Results

with the support pegs. Note that Hudek's test stand astigmatism stayed the same across the mirror rotation. This is a prerequisite of performing the counter-rotate and average method of cancelling test stand astigmatism. Mulherin's test stand astigmatism, on the other hand, changed quite a bit between sets A and B. My guess is that in the A set the pegs had an equal effect, whereas in the B set the left peg was pushing out, while the right peg pulled in. Such a discrepancy in test stand astigmatism causes the counter-rotate and average to give erroneous results—in this case leaving some astigmatism in the final results.

To see what would have happened if Mulherin's results were not thrown off by unruly test stand astigmatism, see Figure 9. In this figure, I have artificially replace the primary astigmatism term of Mulherin's results with the average of the astigmatism terms from Hudek and Eason. I also included the slight rotation to Hudek's results. Notice how Mulherin's Strehl ratio has gone up to .855, which is in line with the others[5].

What about the discrepancy in the first higher-order spherical term (term 15)? I don't have any way to explain this away. It appears to be a genuine difference in the results from the three interferometrists. To get an idea of its significance, we can plot just the spherical terms against each other to make an average radial profile. This is the same way that we would present the results of a Foucault test. Figure 10 shows the results. One piece of information that may related to this discrepancy is that Mulherin performed the interferometry in autocollimation with a flat, which results in a 3" diameter obstruction in the interferograms. Thus, the wavefront model derived from Mulherin's interferograms is an extrapolation in the center region. Both Eason's and Hudek's interferograms include data at the center of the mirror. The symmetric profiles track fairly well for the outer 3/4 of the mirror, and deviate the most in the central 1/4.

Before presenting the final results, I would like to show how I adjust the angle of Hudek's results to line up well with the other wavefront maps and with the support pegs. Figure 11 shows the test stand astigmatism and mirror wavefront before (top) and after (bottom) adjustment. I annotated the mirror wavefront maps with an index mark lined up with the center of the "ridge to the edge" on the Mulherin and Eason wavefront maps. By trial and error, I determined that a counter-clockwise rotation of 6 degrees for set A and 8 degrees for set B gave me the best results. Notice how after the adjustment, the test stand astigmatism lines up with the pegs for sets A and B, and the "ridge"

---

[5]If you don't feel comfortable with my tinkering with the astigmatism term, consider what the results would have been if the astigmatism term had been canceled explicitly, as is often done. In this case, the Strehl ratios would have been .910, .893, and .919, respectively.

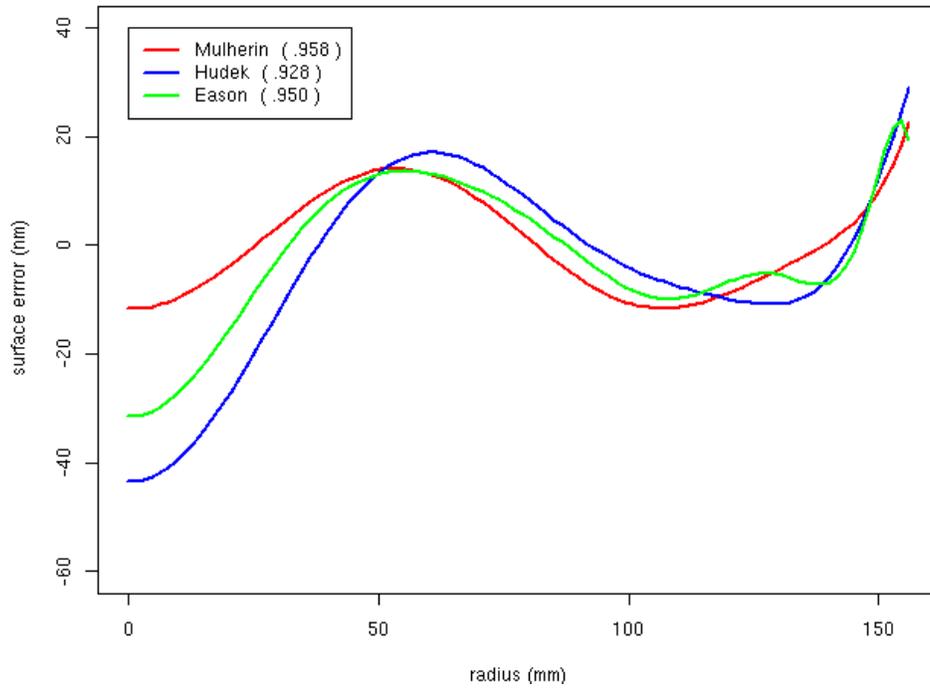Figure 10: Average Radial Profiles

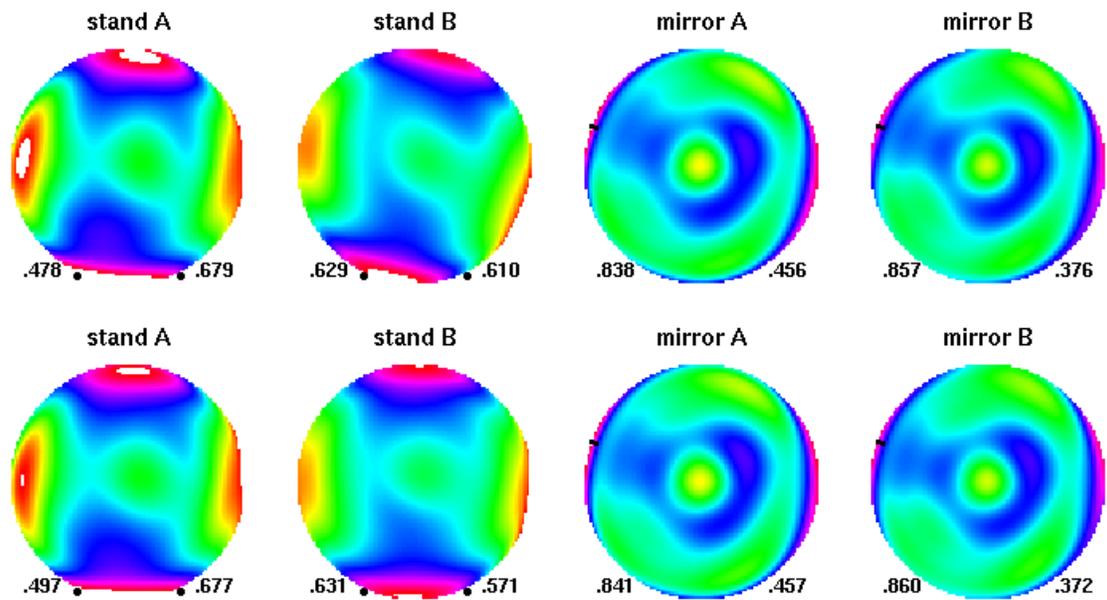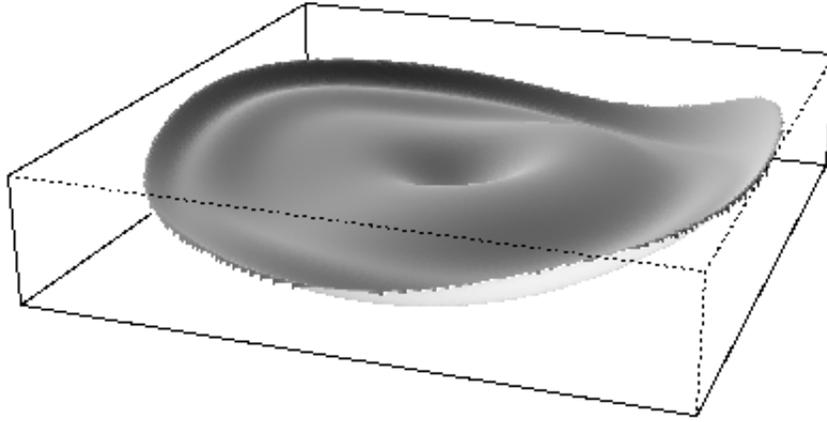
Figure 11: Hudek Rotation Adjustment

Figure 12: Wavefront 3D Surface (Eason)

lines up with the index mark in sets A and B. This rotational difference could have resulted from the placement of the mirror in the test stand, or from a slightly tilted interferometer or camera. Regardless of the cause, this rotational adjustment was not significant in the results, but it allowed a cleaner comparison with the other tests.

Now that we have a stable wavefront map, let's display it another way, and compare it against an independent test. Figure 12 shows a perspective representation of the wavefront, derived from Eason's results. I chose Eason, because it used a fairly large number of Zernike terms, so it shows some good detail. Notice the overall saddle shape, the ring-shaped hill, and the secondary ring just inside the edge. You can also see the ridge that connects the inner ring to the edge. It is somewhat less obvious on this representation, however.

As a final test, we can check whether the wavefront derived from interferometry can predict the appearance of a null Foucault image. Besides taking interferograms, Mulherin captured some Ronchi and Foucault images in autocollimation (null) mode. Figure 13 (left) shows the null Foucault image, in which you can clearly see the turned up edge, the ring just in from the edge, and the central hill[6]. The right image is a simulated null-Foucault image generated from Eason's interferometric results. Other than it being smoother and of higher contrast, there is an overall similarity of features, which is a nice confirmation of the the qualitative results of interferometry.

For reference purposes, the Zernike terms for the results in this paper are given in Table 4 at the end of this report. For table compactness, I left out the higher-level asymmetric terms from Mulherin's data set. The term indices "n" and "m" correspond to Wyant[3]. The index "s" distinguishes between a symmetric term (0), cosine term (1), and sine term (2).

---

[6]If you see the ring just in from the edge as a valley instead of a hill you may need to stare at the image for a while to begin to see it correctly. It helps to imagine that the shadows are cast by a light source that is to the left of the image.

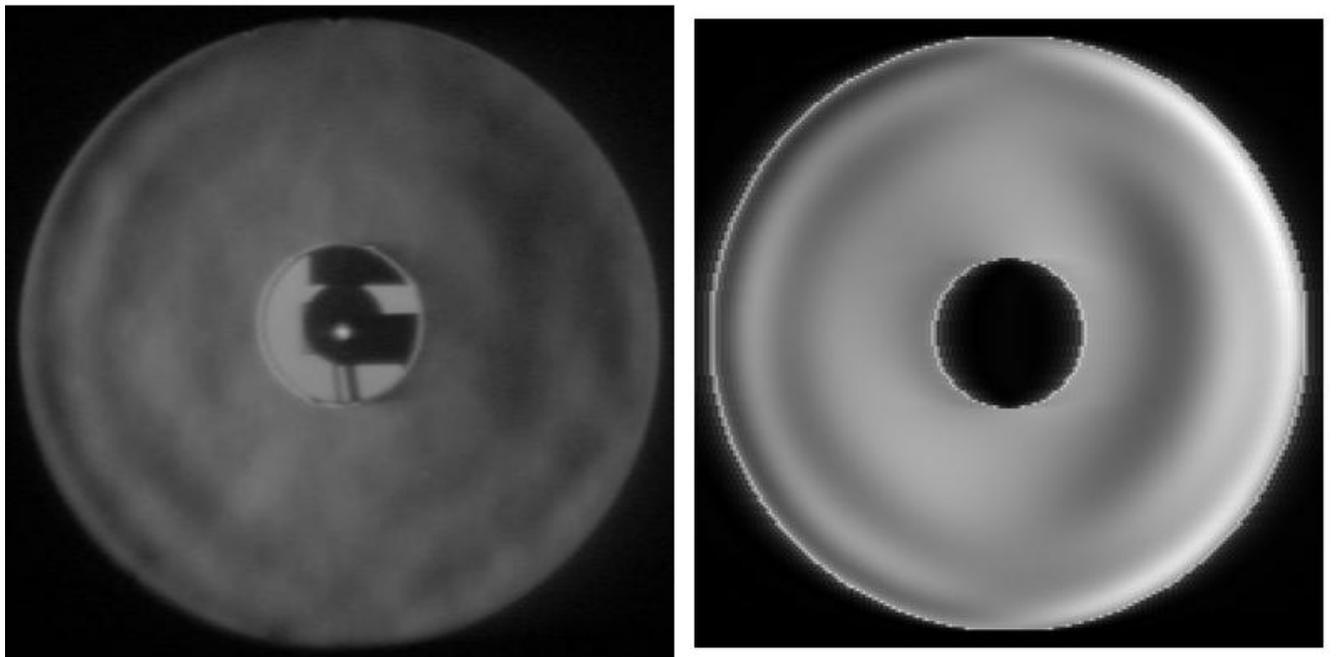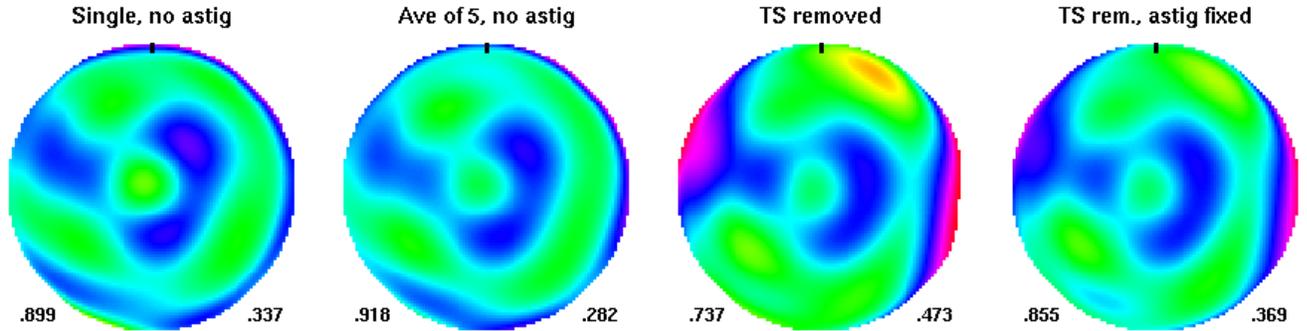Figure 13: Null Foucault Test (actual, simulated)

Figure 14: Reporting Comparison (Mulherin)

Single, no astig	Ave of 5, no astig	TS removed	TS rem., astig fixed
.899 .337	.918 .282	.737 .473	.855 .369

5 Conclusion

All three interferometric analyses came up with very similar results, as shown in Figure 9. I was surprised by how close the results were, considering the challenges faced in testing this optic, and the fact that the tests used such different equipment and techniques. This is a strong argument that interferometry, as practiced by these operators, is capable of accurately capturing the 2D surface of an optic and reporting a reliable RMS error, Strehl ratio, and P-V error.

Nevertheless, I must point out that my analysis, starting with the raw interferograms or with the Zernike terms, was a bit unusual. Typical interferometry would have averaged about five interferograms, and may not have explicitly dealt with test stand astigmatism. Also, the discovery of the high astigmatism term and its explanation required the ability to compare with independent results. It would probably not have been discovered if the only data available were the ten interferograms that Mulherin took. Test stand effects can easily throw off results. Since test stand effects can't be eliminated with thin mirrors, it is probably best to develop a mirror support mechanism with consistent and predictable effects.

I would like to finish with some mild warnings about interferometry reporting. The fact that interferometry was done on an optic does not mean that the results are necessarily accurate. As with any other testing method, interferometry must be done carefully, and its results checked against other methods.

Consider Figure 14 in which I have taken the Zernikes from Mulherin's interferograms and reported the results in various ways. The first frame is from a single interferogram with primary astigmatism cancelled from the results (to cancel test stand astigmatism). The fact that this optic has astigmatism on the glass means that the mirror astigmatism was cancelled along with the test stand astigmatism. Also, a single interferogram frame captures vibration and air turbulence that tend to make the results worse.

The second frame is more realistic. It is an average of the five interferograms from orientation A with astigmatism artificially removed. The results are a little bit higher, but, as with frame one, cancelling astigmatism discards an actual mirror aberration from the results for this example mirror. This kind of analysis is typical—it is a compromise between taking too few interferograms and having the result made worse by noise, and taking twice as many interferograms in order to counter-rotate to cancel test stand astigmatism. If it is known by some other means that the mirror

does not have much astigmatism on the glass, then this method can be accurate, but you must be sure about the status of astigmatism.

Frame three shows the result of the counter-rotate and average to remove test stand astigmatism, but leave the astigmatism present on the glass. The results, as shown before, are much worse. That's because this mirror is a bit astigmatic. In this case, the results are worse than reality (as shown by comparison with the other interferometric analyses), probably as a result of inconsistent test stand deformation. In other words, a counter-rotate and average is not foolproof—it depends on test stand deformation being well-behaved.

Finally, frame four shows the result of frame three, corrected to match the mirror astigmatism of the two other interferometry analyses. I cannot 100% justify this step, but it seems reasonable in light of the other results. I believe frame four to be the most accurate representation of the four in this figure.

References

[1] Ceravolo, Peter. *Interferometry and Telescopes: A practical guide to building and using your own interferometer.* http://www.ceravolo.com/testing/interferometry.pdf.

[2] Rowe, David, *FringeXP* (fringe analysis software). http://www.ceravolo.com/fringe/FringeXP/FringeXP.htm.

[3] Wyant, James C. and Katherine Creath. *Basic Wavefront Aberration Theory for Optical Metrology.* Applied Optics and Optical Engineering, Vol XI. Academic Press, 1992. http://www.optics.arizona.edu/jcwyant/Zernikes/Zernikes.pdf.

[4] Weisstein, Eric W. *Zernike Polynomial.* http://mathworld.wolfram.com/ZernikePolynomial.html.

[5] Wyant, James C. *Zernike Polynomials.* http://www.optics.arizona.edu/jcwyant/Zernikes/ZernikePolynomialsForTheWeb.pdf.

Table 4: Zernike Terms (waves at 550nm)

Indices			Mulherin		Hudek		Eason	
n	**m**	**s**	**A**	**B**	**A**	**B**	**A**	**B**
0	0	0	-2.843	-3.309	0.000	0.000	-2.523	-5.570
1	1	1	-0.153	0.440	-0.003	0.011	2.817	3.991
1	1	2	-3.095	-3.199	-0.000	-0.012	-0.323	4.377
1	0	0	-0.054	0.063	0.003	-0.002	-0.236	1.512
2	2	1	0.247	-0.033	-0.171	-0.300	0.105	-0.086
2	2	2	-0.026	0.140	0.022	0.140	-0.044	0.020
2	1	1	-0.198	-0.086	-0.027	-0.018	0.024	-0.067
2	1	2	-0.056	0.064	0.003	-0.003	0.080	0.066
2	0	0	0.054	0.066	0.037	0.039	0.040	0.054
3	3	1	0.003	-0.048	0.039	-0.022	0.034	-0.050
3	3	2	0.026	0.072	0.033	0.048	0.025	0.015
3	2	1	-0.006	-0.042	-0.021	-0.048	0.005	-0.026
3	2	2	-0.008	0.006	-0.024	0.025	-0.006	0.001
3	1	1	0.066	0.017	0.017	-0.036	0.058	0.025
3	1	2	-0.003	-0.046	-0.036	-0.071	-0.025	-0.055
3	0	0	0.033	0.021	0.102	0.076	0.055	0.060
4	4	1	0.014	0.044	0.017	0.017	-0.007	0.021
4	4	2	-0.025	-0.018	-0.017	-0.012	-0.010	0.003
4	3	1	0.031	0.014	-0.004	0.009	0.012	0.016
4	3	2	-0.023	0.003	-0.002	0.007	-0.013	0.020
4	2	1	0.006	0.011	0.021	0.007	0.005	0.001
4	2	2	0.017	0.008	-0.005	-0.007	0.007	-0.010
4	1	1	0.009	0.002	-0.003	0.024	0.000	0.019
4	1	2	0.034	0.012	0.009	0.014	0.021	-0.003
4	0	0	-0.032	-0.039	-0.037	-0.048	-0.030	-0.028
5	5	1	0.005	0.021	-0.002	0.022	-0.004	0.008
5	5	2	0.004	0.021	0.015	0.007	0.019	0.012
5	4	1	-0.023	-0.041	0.003	-0.004	-0.009	-0.019
5	4	2	0.033	0.020	0.004	0.026	0.023	0.024
5	3	1	-0.045	-0.026	-0.011	-0.030	-0.032	-0.016
5	3	2	0.026	-0.045	0.046	-0.013	0.029	-0.029
5	2	1	0.004	0.031	0.003	0.014	-0.010	0.011
5	2	2	-0.000	-0.001	0.001	-0.009	0.010	0.005
5	1	1	0.000	0.008	-0.039	-0.011	-0.019	-0.001
5	1	2	0.023	0.000	-0.007	0.013	-0.002	0.008
5	0	0	0.033	0.037	0.044	0.041	0.050	0.044
6	0	0	-0.010	-0.000	-0.021	-0.024	-0.018	-0.016
7	0	0	0.000	0.000	0.000	0.000	-0.012	-0.012
8	0	0	0.000	0.000	0.000	0.000	-0.019	-0.028